

Synchrotron X-Ray Characterization of Microstructure Transition and Stress Relaxation of Electroplated Cu upon Self-annealing

Yu-Hsuan Huang (黃禹瑄)¹, Wan-Zhen Hsieh (謝宛蓁)^{1,2}, Cheng-Yu Lee (李承宇)¹, Cheng-Hsien Yang (楊政憲)¹, Shang-Jui Chiu (邱上睿)², Ching-Shun Ku (古慶順)², and Cheng-En Ho (何政恩)^{1,*}

¹Department of Chemical Engineering & Materials Science, Yuan Ze University, Taoyuan City, Taiwan

²National Synchrotron Radiation Research Center, Hsinchu, Taiwan

*E-mail: ceho1975@hotmail.com

Abstract

In-situ analysis of the microstructure transition and stress relaxation of the electroplated copper (Cu) upon self-annealing was conducted via synchrotron monochromatic X-ray diffraction (beamline 17B1, Taiwan Light Source) and white X-ray nanodiffraction (beamline 21A, Taiwan Photon Source). Remarkable Cu grain growth from nanoscale to microscale accompanying with crystallographic reorientation towards (111) + (101) and stress relation towards stress-free state upon self-annealing can be well resolved using the in-situ synchrotron X-ray analysis techniques, which give us an insight into the Cu self-annealing behavior.

Keywords - Cu self-annealing, X-ray diffraction, Synchrotron, Laue diffraction, Hydrostatic/deviatoric strain

Introduction

The deposition of electric circuits/interconnects in printed circuit boards (PCBs) and integrated circuit (IC) devices is usually performed via electroplating Cu. The electroplated Cu films have been reported to appear a remarkable microstructure transition (grain growth) accompanying stress relaxation at room temperature, generally termed Cu self-annealing [1–3]. As the PCB and wafer warpages closely related to the Cu stress relaxation [2], it is therefore of practical importance to in-situ characterize the microstructure transition and strain evolution behaviors of electroplated Cu in its self-annealing procedure.

The complete strain tensor (ε_{ij}) is the sum of the hydrostatic (or mean) strain tensor (δ) and the deviatoric strain tensor (ε'_{ij}), as described in the following equation:

$$\begin{bmatrix} \varepsilon_{11} & \varepsilon_{12} & \varepsilon_{13} \\ \varepsilon_{21} & \varepsilon_{22} & \varepsilon_{23} \\ \varepsilon_{31} & \varepsilon_{32} & \varepsilon_{33} \end{bmatrix} = \begin{bmatrix} \delta & 0 & 0 \\ 0 & \delta & 0 \\ 0 & 0 & \delta \end{bmatrix} + \begin{bmatrix} \varepsilon'_{11} & \varepsilon'_{12} & \varepsilon'_{13} \\ \varepsilon'_{21} & \varepsilon'_{22} & \varepsilon'_{23} \\ \varepsilon'_{31} & \varepsilon'_{32} & \varepsilon'_{33} \end{bmatrix} \quad (1)$$

where the first index (i) indicates the coordinate axis perpendicular to the plane, and the second index (j) indicates that the direction or coordinate axis in which the strain is acting.

X-ray diffraction (XRD) analysis is usually conducted for the strain characterization of a crystalline material. The lattice distortion resulting from a hydrostatic stress can be determined by grazing-incidence X-ray diffraction with monochromatic light through the $\cos^2\alpha\sin^2\psi$ method [4–5]. However, sample tilt would change the scattering volume in the monochromatic XRD analysis. For a local area, the use of white light is a more efficient approach to collect sufficient diffractions necessary to derive the crystallographic information such as grain orientation and strain. It is noted that the white-beam diffraction (alternatively termed Laue diffraction) technique only allows the characterization of the unit-cell distortions (i.e., deviatoric stress), instead of the changes in the unit-cell volume (i.e., hydrostatic stress) [6]. To gain the evolution of both hydrostatic stress (bulk) and deviatoric stress (single grain) stored in electroplated Cu, synchrotron X-ray measurements were performed with monochromatic and white-beam XRD at the beamline 17B1, Taiwan Light Source (TLS) and beamline 21A, Taiwan Photon Source (TPS), respectively.

Experiments

In this study, bare Cu plates (99.99%) were employed as a substrate for Cu electrodeposition. The Cu electrodeposition was carried out in a Haring cell under a fixed plating current density (j) (2 A/dm²) at room temperature. The thickness of electroplating Cu (δ_{Cu}) was controlled to be 20(±2) μm. To characterize the microstructure transition and stress relaxation relative to Cu self-annealing time (t), the synchrotron X-ray measurements were performed. For monochromatic XRD analysis (beamline 17B1, TLS), the beam energy was 8 keV with a wavelength (λ) of 1.54975 Å and a spot size of 500–700 μm. The sample was mounted on an eight-circle goniometer, where the film tilted angle (Ψ) ranges from -19° to 41°. A low grazing angle of X-ray incidence (γ) was set at 1°. For Laue diffraction (beamline 21A, TPS), synchrotron white X-ray nanodiffraction with a focused spot size of 70 nm × 70 nm and an energy range of 5–30 keV was employed to characterize of crystallographic transition and the corresponding deviatoric components.

Results and Discussion

Monochromatic XRD ($\cos^2\alpha\sin^2\psi$ method)

Fig. 1(a) shows synchrotron monochromatic XRD spectra of the electroplated Cu at different t , where $\Psi = -19^\circ$. Insignificant (200) peaks were observed in the early stage of Cu self-annealing ($t = 0-4$ h), suggesting that the weak crystallites existed during the incubation time period for the onset of grain growth. By increasing t from 4 h to 14 h, the diffraction intensities of the Cu (200) peaks significantly increased, while the full width at half maximum (FWHM) decreased from 0.493° to 0.055°. A increase in the diffraction intensity and a decrease in the FWHM value confirmed that a noticeable recrystallization/grain growth indeed occurred in the as-deposited Cu in a few hours even at room temperature.

Based on the results of Fig. 1, the hydrostatic stress of electroplated Cu can be calculated through the $\cos^2\alpha\sin^2\psi$ method [4–5]:

$$\frac{d_{\alpha\psi} - d_0}{d_0} = \frac{1+\nu}{E} \sigma \cos^2 \alpha \sin^2 \psi + \frac{1+\nu}{E} \sigma \sin^2 \alpha - \frac{2\nu}{E} \sigma \quad (2)$$

where $d_{\alpha\psi}$ and d_0 represent the lattice spacing obtained from electroplated Cu and lattice spacing of the stress-free Cu (1.8 Å), respectively. E and ν represent Young's modulus (130 GPa) and Poisson's ratio (0.34) of Cu, respectively [7]. σ represents hydrostatic stress. $\alpha = \gamma - \theta$, where θ is the diffraction angle (Fig. 1).

In this study, the sample was tilted in different Ψ angles, where $\Psi = -19^\circ$ to 41° . $d_{\alpha\Psi}$ can be calculated through $d_{\alpha\Psi} = \lambda/(2 \times \sin\theta)$. Insertion of the above parameters into Eq. (2) yields σ , and the calculated σ as a function of t were plotted in Fig. 1(b). The hydrostatic stress was approximately 150 MPa at the as-deposited state ($t = 0$ h) and then increased to approximately 300–450 MPa after $t = 6$ h, indicating that the hydrostatic distortion would increase after self-annealing.

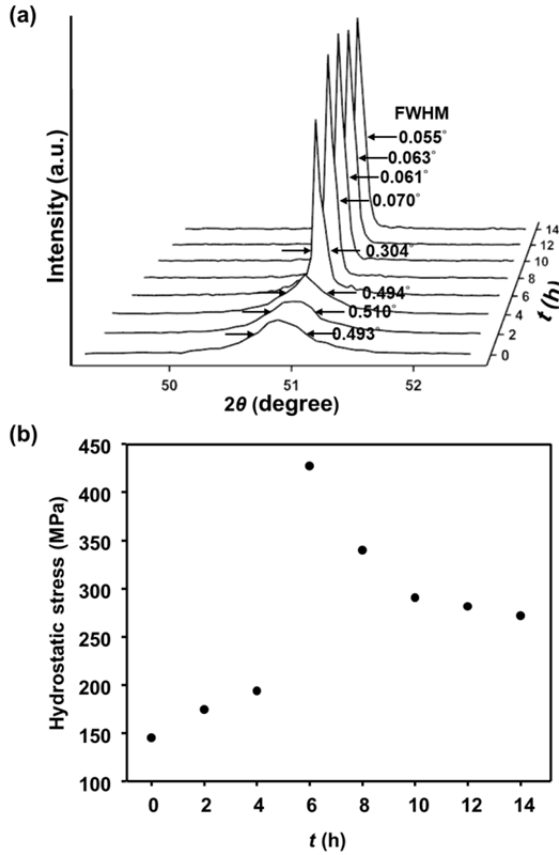


Fig. 1. (a) In-situ synchrotron X-ray diffraction spectra of electroplating Cu upon self-annealing.; (b) Hydrostatic stress of electroplated Cu as a function of t .

Laue Diffraction Analysis

Fig. 2(a)–(f) shows the orientation maps of the electroplated Cu at $t = 4$ h (a), 6 h (b), 8 h (c), 10 h (d), 16 h (e), and 20 h (f), which was determined using white X-ray nanodiffraction that provides crystallographic information upon self-annealing. Each color corresponds to individual crystallographic orientation, as represented in the stereographic triangle. The color red, blue, and green were assigned to the $\langle 001 \rangle$, $\langle 111 \rangle$, and $\langle 101 \rangle$ crystallographic direction, respectively. The variation in color of the neighboring pixels at the early stage of self-annealing ($t = 4$ – 6 h) implies that a random distribution in Cu crystallographic orientation with a nanocrystalline structure. Remarkable Cu grain growth was observed as t increased to 8 h (Fig. 2c), where the orientation maps approximately exhibit green and blue, indicating that $\langle 101 \rangle$ and $\langle 111 \rangle$ were the predominant orientation after Cu grain growth. A fully developed microstructure can be achieved after self-annealing of 10 h.

Fig. 2(a')–(f') shows the deviatoric stress distribution along the Cu deposition direction (σ_{zz}) corresponding to 2(a)–(f'), respectively. The X-ray strain measurements utilize the shifts/distortions in diffraction peaks and provide elastic strains (ϵ). The deviatoric stress maps approximately exhibit red and blue at $t = 4$ – 8 h, indicating the existence of noticeable compressive and tensile stresses along the Cu deposition direction at the early stage of self-annealing. Fig. 3 summarizes the deviatoric stress of electroplated Cu against t . The deviatoric stress tended to zero after $t = 10$ h (Fig. 2d'–f'), corresponding to the fully developed microstructure obtained in Fig. 2(d)–(f).

The above synchrotron studies (monochromatic XRD and Laue diffraction) showed that both hydrostatic and deviatoric distortions of electroplated Cu was relaxed towards tensile direction and a stable microstructure/stress could be obtained after self-annealing of 10 h.

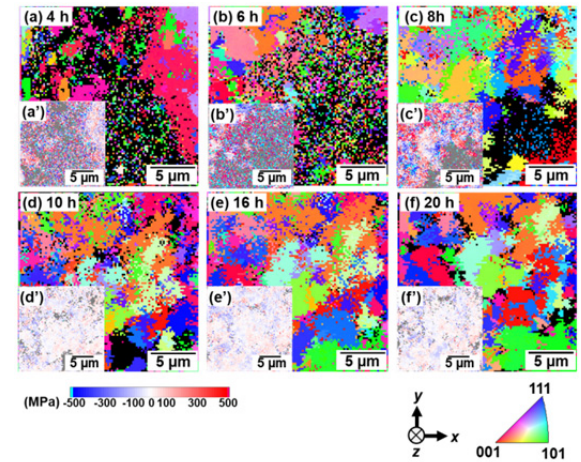


Fig. 2. (a)–(f) Crystallographic orientation maps of electroplated Cu at $t =$ (a) 4 h, (b) 6 h, (c) 8 h, (d) 10 h, (e) 16 h, (f) 20 h. (a')–(f') Deviatoric stress maps (σ_{zz}) corresponding to (a)–(f), respectively. The dark/gray pixels were the unresolved area.

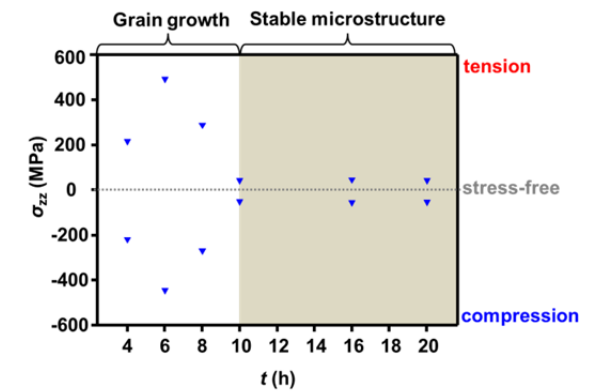


Fig. 3. Deviatoric stress (σ_{zz}) of electroplated Cu as a function of t .

Acknowledgments

This study was supported by the Ministry of Science and Technology (R.O.C.) through Grant Nos. MOST108-2221-E-155-032 & MOST106-2119-M-213-001-MY3

References

- [1] M. Stangl, M. Liptak, A. Fletcher, J. Acker, J. Thomas, H. Wendrock, S. Oswald, K. Wetzig, *Microelect. Eng.* 85 (2008) 534–541.
- [2] C.H. Yang, S.P. Yang, B. C. Huang, C.Y. Lee, H.C. Liu, C.E. Ho, *Surf. Coat. Technol.* 364 (2019) 383–391.
- [3] C.E. Ho, C.C. Chen, M.K. Lu, Y.W. Lee, Y.S. Wu, *Surf. Coat. Technol.* 303 (2016) 86–93.
- [4] A.N. Wang, C.P. Chuang, G.P. Yu, J.H. Huang, *Surf. Coat. Technol.* 262 (2015) 40–47.
- [5] C.H. Ma, J.H. Huang, H. Chen, *Thin Solid Films* 418 (2002) 73–78.
- [6] N. Tamura, A.A. MacDowell, R. Spolenak, B.C. Valek, J.C. Bravman, W.L. Brown, R.S. Celestre, H.A. Padmore, B.W. Batterman, J.R. Patel, *J. Synchrotron Rad.* 10 (2003) 137–143.
- [7] L.B. Freund, S. Suresh, “Thin Film Materials: Stress, Defect Formation, and Surface Evolution,” Cambridge University Press, 2004.